PACKET TRAFFIC DYNAMICS NEAR ONSET OF CONGESTION IN DATA COMMUNICATION NETWORK MODEL*

Anna T. Lawniczak

Department of Mathematics and Statistics & Guelph-Waterloo Physics Institute
The Biophysics Interdepartmental Group (BIG), University of Guelph
Guelph, Ontario N1G 2W1, Canada

Xiongwen Tang

Department of Statistics and Actuarial Science
University of Iowa, Iowa City, Iowa 52242-1409, USA

(Received March 28, 2006)

Dedicated to Professor Peter Talkner on the occasion of his 60-th birthday.

The dominant technology of data communication networks is the Packet Switching Network (PSN). It is a complex technology organized as various hierarchical layers according to the International Standard Organization (ISO) Open Systems Interconnect (OSI) Reference Model. The Network Layer of the ISO OSI Reference Model is responsible for delivering packets from their sources to their destinations and for dealing with congestion if it arises in a network. Thus, we focus on this layer and present an abstraction of the Network Layer of the ISO OSI Reference Model. Using this abstraction we investigate how onset of traffic congestion is affected for various routing algorithms by changes in network connection topology. We study how aggregate measures of network performance depend on network connection topology and routing. We explore packets traffic spatio-temporal dynamics near the phase transition point from free flow to congestion for various network connection topologies and routing algorithms. We consider static and adaptive routings. We present selected simulation results.

PACS numbers: 89.20.Ff, 89.20.Hh, 89.75.–k, 89.75.Kd,

* Presented at the XVIII Marian Smoluchowski Symposium on Statistical Physics, Zakopane, Poland, September 3–6, 2005.

1. Introduction

A data communication network of packet switching type consists of a number of nodes (*i.e.*, *routers* and *hosts*) that are interconnected by communication links. The purpose of packet switching network (PSN) is to transmit messages from their sources to their destinations. The PSN owes its name to the fact that in this type of network each message is partitioned into smaller units of information called *packets*. Packets are transmitted individually from their sources to their destinations via a number of *switching nodes*, called *routers*, and communication links interconnecting them. Since packets may arrive to their destinations via different routes and out of order the message may have to be rebuilt at the destination. Examples of PSN include the Internet, wide area networks (WANs), local area networks (LANs), wireless communication networks, ad-hoc networks, or sensor networks.

There is vast engineering literature devoted to PSNs, see [1–6]. Wired PSNs are described by the ISO (International Standard Organization) OSI (Open Systems Interconnect) 7 layer Reference Model [1–3,7]. The Network Layer of the OSI Reference Model of wired PSNs is responsible for routing packets across the network from their sources to their destinations and for control of congestion in data networks. Thus, the Network Layer plays an essential role in the packet traffic dynamics. These dynamics may be very complex and it is not well understood how they are affected by changes in network connection topology for various routing algorithms [8–16]. For future design of PSNs, efficient control of their congestion and improvements in their defense strategies, it is important to improve the understanding of packet traffic dynamics ([16] and references therein). With this goal in mind at different levels of abstraction various models of PSNs have been proposed and analyzed (see, [8–27] and the articles therein). The engineering community uses very detailed and complex simulation models. Often these models are too specific to capture and study generic properties of realistic data networks. Simplified models of PSNs within the statistical physics community are able to capture some dynamical properties of packet traffics of real data networks without incorporating the details of routing protocols and realistic network connection topologies into these models [8–47].

In our research we use an abstraction of the Network Layer developed in [15,20,21] and a C++ simulator, called Netzwerk-1 described in [15,20,21, 26]. The PSN model used in our research is concerned mainly with packets and their routing as the Network Layer in real PSN networks. Our PSN simulation model [15, 20, 21], even though it is still abstract, incorporates some details of routing protocols and network connection topologies. Thus, our model fills the gap between the detailed models and the simplified ones.

Continuing our work of [9,12,15,20,22,28–36] we investigate how various network performance indicators depend on network connection topology and routing algorithms. We explore the packet traffic dynamics near phase transition point from free flow to congestion for static and adaptive routing algorithms.

2. Description of Packet Switching Network model

In our PSN model (see [15] and [20]) the lengths of all messages are restricted to one packet carrying only the following information: time of creation, destination address, and number of hops taken. In this PSN model each node can perform the functions of a *host* and a *router*. Hosts generate and receive packets and routers store and forward packets on their route from source to destination. At each node packets are created randomly and independently with probability λ, called *source load*. To store the packets each node maintains one incoming and one outgoing queue. The outgoing queues are assumed to be of unlimited length and operate according to first-in, first-out policy. At each time step each node, independently from the other nodes, routes the packet from the head of its outgoing queue to the next node on the packet's route. A discrete time, synchronous and spatially distributed network algorithm implements the creation and routing of packets, see [15] and [20].

In our PSN model network connection topology is represented by a weighted directed multi-graph $\mathcal{L}$ where each vertex represents a node and each pair of parallel edges oriented in opposite directions represents a communication link. A weight assigned to each directed edge of the multi-graph $\mathcal{L}$ represents a packet transmission cost along this edge. Thus parallel edges do not necessarily share the same cost.

In each instance of PSN model set-up all edge costs are computed using the same type of *edge cost function (ecf)* that is either the edge cost function called *One* (ONE), or *QueueSize* (QS), or *QueueSizePlusOne* ($QSPO$). Edge cost function ONE assigns a value of "one" to each edge in the multi-graph $\mathcal{L}$. It is a static cost because the edge costs do not change during the course of a simulation. This results in a *static routing*. The edge cost function QS assigns to each edge in the multi-graph $\mathcal{L}$ a value equal to the length of the outgoing queue at the node from which the edge originates. The edge cost function $QSPO$ assigns a value that is the sum of a constant "one" plus the length of the outgoing queue at the node from which the edge originates. The costs QS and $QSPO$ are derived for each edge from load of the router from which the edge originates. The routing decisions made using QS or $QSPO$ edge cost function are based on the current state of the network simulation. They imply *adaptive* or *dynamic routing* where packets have the ability to avoid congested nodes during the PSN model simulation.

In our PSN model, each packet is transmitted via routers from its source to its destination according to the routing decisions made independently at each router and based on a *minimum least-cost criterion*. In the case of edge cost function ONE this results in the *minimum hop routing* (*minimum route distance*) and in the case of edge cost function QS or $QSPO$ this results in the *minimum route length*, see [1] and [6]. Our PSN model uses *full-table routing*, that is, each node maintains a routing table of least path cost estimates from itself to every other node in the network. When the edge cost function QS or $QSPO$ is used, the routing tables are updated at each time step using a distributed version of Bellman–Ford least-cost algorithm [6]. In both cases of edge cost functions, QS and $QSPO$, the path costs stored in the routing tables are only estimates of the actual least path costs across the network because only local information is exchanged and updated at each time step. The routing tables do not need to be updated when the static cost ONE is assigned to each edge of the multi-graph $\mathcal{L}$ because this cost does not change during a simulation. It is independent of the state of the network. The routing tables are calculated only at the beginning and the cost estimates are the precise least-costs, see [15] and [20].

In the PSN model time is discrete and we observe its state at the discrete times $k = 0, 1, 2, \dots, T$, where T is the final simulation time. At time $k = 0$, the set-up of the PSN model defined by the choice of network connection topology type, edge cost function type, and source load is initialized with empty queues and the routing tables are computed using the centralized Bellman–Ford least-cost algorithm [6]. The discrete time, synchronous and spatially distributed PSN model algorithm consists of the sequence of five operations advancing the simulation time from k to $k+1$. These operations are:

1. *Update routing tables.* The routing tables of the network are updated in a distributed manner, if the PSN model set-up uses edge cost function QS or $QSPO$.
2. *Create and route packets.* At each node, independently of the other nodes, a packet is created randomly with source load λ. Its destination address is randomly selected among all other nodes in the network with uniform probability. The newly created packet is placed in the incoming queue of its source node. Further, each node, independently of the other nodes, takes the packet from the head of its outgoing queue (if there is any), determines the next node on a least-cost route to its destination (if there is more than one possibility then selects one at random with uniform probability), and forwards this packet to this node. Packets, which arrive at a node from other nodes during this step of the algorithm, are destroyed immediately if this node is their destination, otherwise they are placed in the incoming queue.

3. *Process incoming queue.* At each node, independently of the other nodes, the packets in the incoming queue are randomized and inserted at the end of the outgoing queue.
4. *Evaluate network state.* Various statistical data about the state of the network at time k are gathered and stored in time series.
5. *Update simulation time.* The time k is incremented to $k+1$.

The detailed description of this algorithm and its software implementation is provided in [15, 20, 21] and [26].

3. Packet traffic dynamics

In order to study packet traffic dynamics engineers and network operators use various network performance indicators like *critical source load*, *throughput*, *number of packets in transit*, *average delay time of all packets delivered*, *average path length*, *round trip return time*, or *latency*, see [1–6,15]. These network performance indicators provide aggregate information about packet traffic. Our study shows that the network performance indicators may be almost identical for different PSN model set-ups. However, these PSN model set-ups may exhibit very different spatio-temporal packet traffic dynamics. Thus, the aggregate measures of network performance may provide little insight into packet traffic patterns and their spatial and temporal dynamics. For the improvements in design and management of PSNs such information is important, for example to avoid over- or under-utilizations of some network routers that may result from coupling of network connection topology with routing algorithm, *i.e.*, from a PSN internal dynamics. Providing such information requires development of new methodologies that include modeling, simulation, data mining, visual data mining, real-time data base techniques [16, 48, 49].

Our research contributes to the investigation of spatio-temporal packet traffic dynamics in PSNs. We study how these dynamics are affected by coupling of network connection topology with routing algorithms (specified by a selection of edge cost function) for source loads close to the phase transition point of each PSN model set-up. We study how small changes in network connection topology may affect packet traffic patterns.

As a case study we consider network connection topologies that are isomorphic to either $\mathcal{L}^{\mathrm{p}}_{\Box}(16,l)$ (*i.e.*, isomorphic to a two-dimensional periodic square lattice with $L=16$ nodes in the horizontal and vertical directions and with l additional links added to this square lattice) or $\mathcal{L}^{\mathrm{p}}_{\triangle}(16,l)$ (*i.e.*, isomorphic to a two-dimensional periodic triangular lattice with $L=16$ nodes in the horizontal and vertical directions and with l additional links added to this triangular lattice). Notice, that if a sufficient number $l_s = l_1 + l_2$ of additional links is added to $\mathcal{L}^{\mathrm{p}}_{\square}(16,l)$, with l_1 links added in a proper way, then one obtains a network connection topology of the type $\mathcal{L}^{\mathrm{p}}_{\triangle}(16,l+l_2)$, *i.e.* $\mathcal{L}^{\mathrm{p}}_{\square}(16,l+l_1+l_2)=\mathcal{L}^{\mathrm{p}}_{\triangle}(16,l+l_2)$. Fig. 1 illustrates how to obtain a non-periodic or periodic triangular lattice from a square lattice. In the presented simulations of PSN model set-ups all links are static for the duration of each simulation run and $L=16$, and $l=0$, or 1.

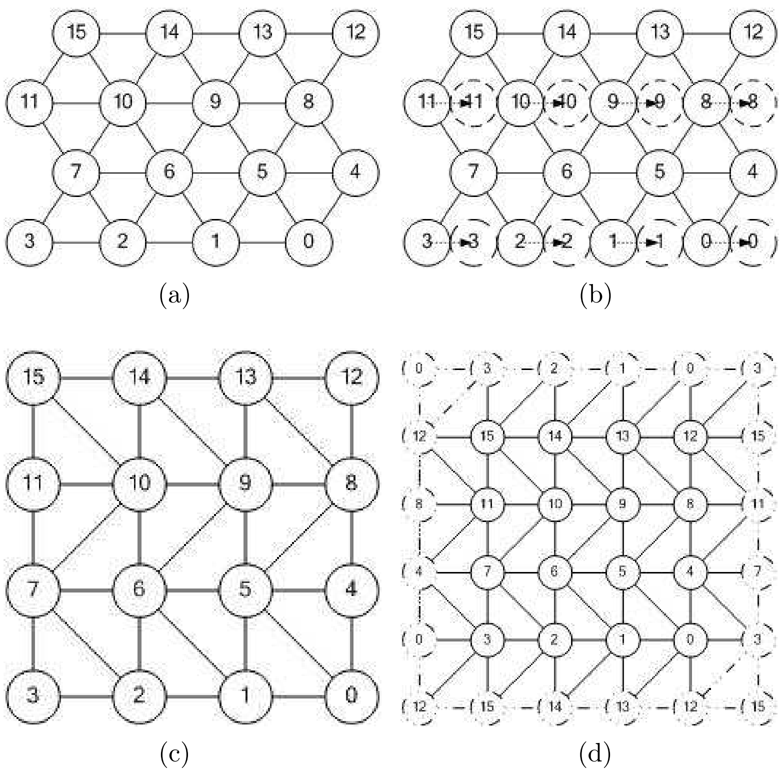

Fig. 1. Illustration of the relationship between non-periodic triangular lattice and non-periodic square lattice with extra links (a), (b), and (c). Figure (d) shows a periodic 4×4 square lattice with extra links isomorphic to a periodic triangular lattice.

We say that $\mathcal{L}^{\mathrm{p}}_{\square}(16,0)$ and $\mathcal{L}^{\mathrm{p}}_{\triangle}(16,0)$, that is, the regular network connection topologies are *undecorated* and we say that they are *decorated* if an extra link is added to each of them, that is, they are of the type $\mathcal{L}^{\mathrm{p}}_{\square}(16,1)$ or $\mathcal{L}^{\mathrm{p}}_{\triangle}(16,1)$. We use the following convention when we want to specify additionally what type of an edge cost function the PSN model set-up is using, namely, $\mathcal{L}^{\mathrm{p}}_{\square}(16,1,ecf)$ and $\mathcal{L}^{\mathrm{p}}_{\triangle}(16,1,ecf)$, where $l=0$ or 1, and $ecf=ONE$, or QS, or $QSPO$.

3.1. Aggregate information about packet traffic

In this section we analyze the behavior of the following network performance indicators: *number of packets in transit* (NPT), *reduced number of packet in transit* (*reduced* NPT), *average delay time of all packets delivered* ($ADTPD$), *critical source load* (CSL) and *throughput* for the PSN model set-ups $\mathcal{L}^{\mathrm{p}}_{\square}(16, l, ecf)$ and $\mathcal{L}^{\mathrm{p}}_{\triangle}(16, l, ecf)$, where $l = 0$ or 1, and $ecf = ONE$, or QS, or $QSPO$. These indicators are some of the most important network performance indicators used to assess PSN performance [1–6,15,16]. Because time is discrete in our algorithmic simulation model of PSN, "t" stands for a discrete time step of a simulation run, in the following definitions of the network performance indicators.

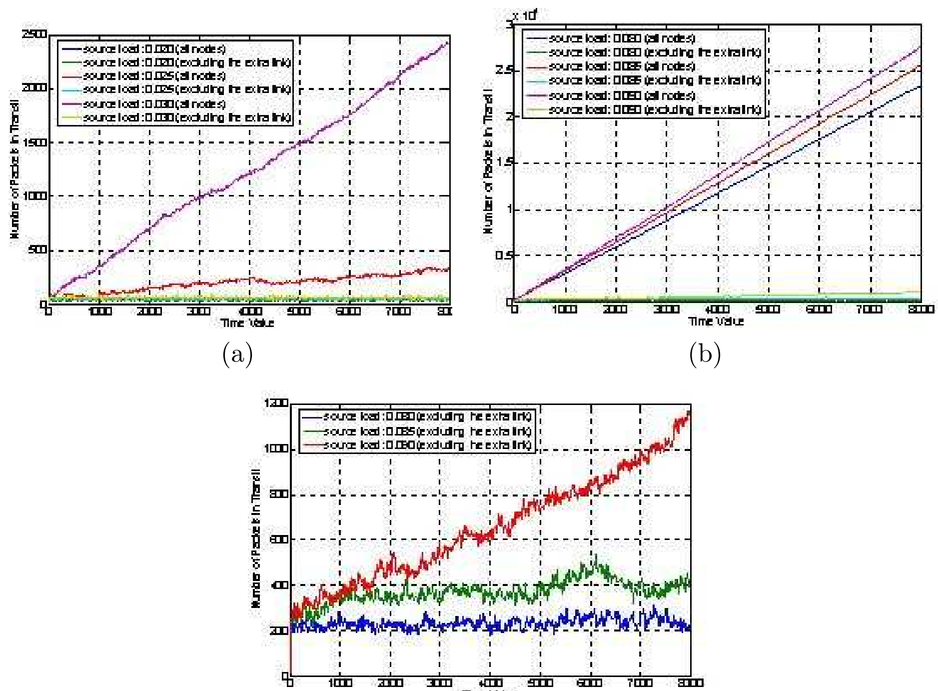

(a) (b) (c)

Fig. 2. Plots of NPT (outgoing queue sizes sum over all nodes) and *reduced* NPT (outgoing queue sizes sum over all nodes except two end nodes of the extra link) as a function of time for various source loads for the PSN model set-up $\mathcal{L}^{\mathrm{p}}_{\square}(16, 1, ONE)$. Graphs of NPT and *reduced* NPT on (a), (b) and (c) are plotted at every 10 time steps, up to 8000, for source loads (a) 0.020, 0.025, 0.035 (b) 0.080, 0.085, 0.090 and for *reduced* NPT only in (c) for source loads 0.080, 0.085, 0.090.

The *N(t)* stands for the *number of packets in transit* (*NPT*, sometimes called *total NPT*) at time t, that is, it is the total number of packets in transit in the network at time t. Thus, $N(t)$ is the sum of all the packets in the out-going queues of the PSN model set-up at time $k = t$. This indicator represents a direct measure of how heavy the network traffic is: in the case of congestion $N(t)$ fluctuates around an increasing trend that is increasing with time, otherwise $N(t)$ fluctuates around some constant value after some initial transient time. The graphs of $N(t)$ of PSN model set-up $\mathcal{L}^{\mathrm{p}}_{\square}(16, 1, ONE)$ and various values of source load λ can be seen from Fig. 2. The *reduced number of packet in transit* (*reduced NPT*) is calculated by summing the outgoing queue sizes of selected nodes of the PSN model set-up. In Fig. 2 the *reduced NPT* is calculated by excluding the nodes of the extra link, that is, it is the *total NPT* but without counting the packets of the outgoing queues of the two end nodes of the extra link. We observe that the *reduced NPT* fluctuates around an increasing trend with an increase of time but for much higher values of source load λ than the *total NPT*. This means that the PSN model set-up $\mathcal{L}^{\mathrm{p}}_{\square}(16, 1, ONE)$ becomes heavily locally congested already for small values of source load λ and becomes *globally congested* for much higher values of source load λ. The reason for the build up of the local congestion is that many packets utilize a shortcut provided by an extra link regardless of how congested the end nodes of this link are. This is because in the PSN model using *ecf ONE,* that is a static routing, there is no built-in routing mechanism to avoid congested nodes. Thus, local congestion builds up very fast affecting readings of the *total NPT*. Similar behavior of graphs *total NPT* and *reduced NPT* was observed for PSN model set-ups $\mathcal{L}^{\mathrm{p}}_{\triangle}(16, 1, ONE)$.

The *average delay time of all packets delivered* (*ADTPD*) at a simulation time $k = t$ is calculated as the sum of delay times of all the packets that have reached their destinations before time t, divided by the total number of packets delivered in the time interval $[0, t]$, see [15]. The delay time of a packet is defined as $\tau = t_{\mathrm{d}} - t_{\mathrm{c}}$, where t_{d} is the *delivery time* of the packet to its destination (the simulation cycle number in which the packet has been delivered) and t_{c} is the packet's creation time. Thus, the network performance indicator *ADTPD* tells us how long, on average, it takes for a packet to reach its destination in a time interval $[0, t]$ of the network operation.

One of the very important network performance indicators is the *critical source load*. It characterizes a *phase transition point* separating *congestion-free* state from *congested state* of PSN. The phase transition from *free flowing traffic state* of a network where packets reach their destinations in a timely manner to *congested state* was observed in empirical studies of PSNs [38] and motivated further research (*e.g.*, [8–47]). Understanding the dynamics of the phase transition has practical implications that may lead to more efficient designs of PSNs.

In our PSN model, for each family of network set-ups, which differ only in the value of the source load λ, values of $\lambda_{\mathrm{sub-c}}$ for which packet traffic is congestion-free are called *sub-critical source loads* while values $\lambda_{\mathrm{sup-c}}$ for which traffic is congested are called *super-critical source loads.* The *critical source load* λ_{c} is the largest sub-critical source load. For a given PSN model set-up determination of the critical source load includes studying, among other indicators, time evolution of $N(t)$ (*i.e.*, the *number of packets in transit* (NPT)) for various source loads, see Fig. 2. We observe that for $\lambda_{\mathrm{sub-c}}$ source load values $N(t)$ fluctuate around some constant value after some initial transient time and for $\lambda_{\mathrm{sup-c}}$ source load values $N(t)$ fluctuate around an increasing trend that is increasing with time. Details about how the critical source load is estimated in our PSN model simulations are provided in [15]. For the PSN model set-ups considered here the estimated critical source load values are provided in Table I.

TABLE I

Critical source load values.

ecf	λ_{c} of $\mathcal{L}^{\mathrm{p}}_{\square}(16,0)$	λ_{c} of $\mathcal{L}^{\mathrm{p}}_{\square}(16,1)$	λ_{c} of $\mathcal{L}^{\mathrm{p}}_{\triangle}(16,0)$	λ_{c} of $\mathcal{L}^{\mathrm{p}}_{\triangle}(16,1)$
ONE	0.115	0.020	0.140	0.030
QS	0.120	0.125	0.155	0.160
QSPO	0.120	0.125	0.155	0.160

We observe that for PSN model set-ups $\mathcal{L}^{\mathrm{p}}_{\square}(16,0,ecf)$, where $ecf = QS$ or $QSPO$, the critical source loads have the same value (at the precision level of our estimation) and this value is only slightly larger than the critical source load of PSN model set-up $\mathcal{L}^{\mathrm{p}}_{\square}(16,0,ONE)$. The same holds true for PSN model set-ups $\mathcal{L}^{\mathrm{p}}_{\triangle}(16,0,ecf)$, where $ecf = ONE$ or QS or $QSPO$. We also observe that the addition of an extra link decreases significantly the critical source loads for PSN model set-ups using edge cost function *ONE* but has almost no effect on them for the PSN model set-ups using edge cost function *QS* or *QSPO.* The extensive study of effects of network connection topology, edge cost function type, and mode of routing table update on critical source load values in the PSN model under consideration is reported in [15,29–34]. Here we discuss how network performance indicators *number of packets in transit*, *throughput* and *average delay time of all packets delivered* evaluated at a given time $T = 6400$ depend on source load λ.

Another very important network performance indicator is *throughput.* It measures the rate at which a network delivers packets to their destinations. Thus, *throughput* of each PSN model set-up at simulation time t is calculated by taking the time-average of a total number of packets delivered to their destinations up to time t.

Fig. 3 and Fig. 4 display graphs of *throughput* as a function of source load λ of PSN model set-ups $\mathcal{L}^{\mathrm{p}}_{\Box}(16, l, ecf)$ and $\mathcal{L}^{\mathrm{p}}_{\triangle}(16, l, ecf)$, respectively, where $l = 0$ or 1, and $ecf = ONE$ or QS or $QSPO$, calculated from simulation runs up to $T = 6400$ updates. We observe that graphs of *throughputs* of PSN model set-ups $\mathcal{L}^{\mathrm{p}}_{\Box}(16, 0, ecf)$ with $ecf = ONE$ or QS or $QSPO$ are almost identical, see (a) in Fig. 3. The same holds true for PSN model set-ups $\mathcal{L}^{\mathrm{p}}_{\triangle}(16, 0, ecf)$ with $ecf = ONE$ or QS or $QSPO$, see (a) in Fig. 4. For each type of network connection topology *throughput* graphs for various ecfs attain their maximum at almost the same value of source load λ_{T} that is a bit larger than the corresponding critical source loads λ_{c}. We observe that the rate of increase of *throughput* graphs is constant for source loads λ lower than λ_{T}.

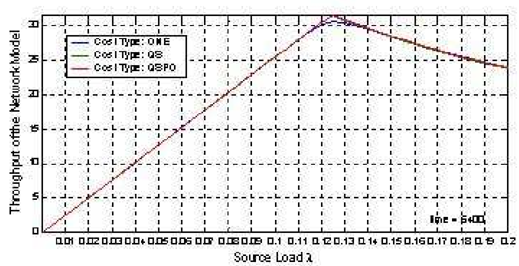

(a)

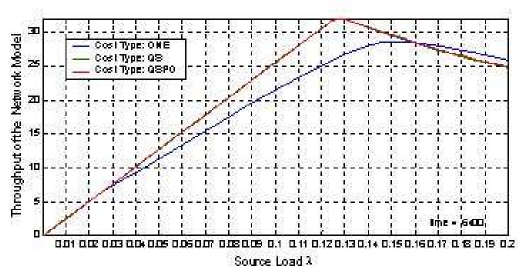

(b)

Fig. 3. Plots of *throughput* of the PSN model set-up with network connection topology $\mathcal{L}^{\mathrm{p}}_{\Box}(16, 0)$ in (a) and $\mathcal{L}^{\mathrm{p}}_{\Box}(16, 1)$ in (b) and edge cost function ONE blue graphs, QS green graphs and $QSPO$ red graphs, at simulation time $T = 6400$.

By comparing the graphs of figure (a) with those of figure (b), respectively in Fig. 3 and Fig. 4, we notice that addition of an extra link to the network connection topology has very little effect on *throughput* of PSN

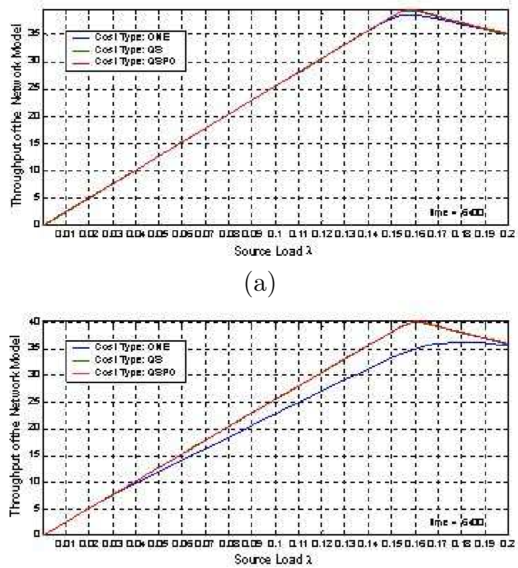

(a)

(b)

Fig. 4. Plots of *throughput* of the PSN model set-up with network connection topology $\mathcal{L}^{\mathrm{p}}_{\triangle}(16,0)$ in (a) and $\mathcal{L}^{\mathrm{p}}_{\triangle}(16,1)$ in (b) and edge cost function ONE blue graphs, QS green graphs and $QSPO$ red graphs, at simulation time $T = 6400$.

model set-ups using edge cost function *QS* or *QSPO*. However, it has a significant effect on *throughput* in the case of PSN model set-ups using the edge cost function *ONE*. Addition of an extra link to the network connection topologies $\mathcal{L}^{\mathrm{p}}_{\square}(16,0)$ and $\mathcal{L}^{\mathrm{p}}_{\triangle}(16,0)$ decreases the maximum value of *throughput* of each PSN model set-up $\mathcal{L}^{\mathrm{p}}_{\square}(16,1,ONE)$ and $\mathcal{L}^{\mathrm{p}}_{\triangle}(16,1,ONE)$. The respective source load value λ_{T} at which *throughput* attains its maximum, that is about 0.155 for the PSN model set-up $\mathcal{L}^{\mathrm{p}}_{\square}(16,1,ONE)$ and it is about 0.170 for the PSN model set-up $\mathcal{L}^{\mathrm{p}}_{\triangle}(16,1,ONE)$, is much higher than the corresponding critical source load value $\lambda_{\mathrm{c}} = 0.020$ for $\mathcal{L}^{\mathrm{p}}_{\square}(16,1,ONE)$, and $\lambda_{\mathrm{c}} = 0.030$ for $\mathcal{L}^{\mathrm{p}}_{\triangle}(16,1,ONE)$. This is due to the significant build up of local congestion at the end nodes of an extra link. This build-up happens already for very small source load values before the network becomes globally congested at much higher source load values, as can be seen from Fig. 2 in the case of PSN model set-up $\mathcal{L}^{\mathrm{p}}_{\square}(16,1,ONE)$. This build-up of local congestion may also explain why for source load values lower than λ_{T} the rate of increase of *throughput* is not constant any longer. We observed similar qualitative behaviors of *throughput* graphs for PSN model set-ups with network connection topologies of different size and type (*e.g.*, non-periodic square lattices or non-periodic triangular lattices).

Fig. 5 and Fig. 6 display graphs of *number of packet in transit* (NPT) as a function of source load λ of PSN model set-ups $\mathcal{L}^{\mathrm{p}}_{\Box}(16, l, ecf)$ (Fig. 5) and $\mathcal{L}^{\mathrm{p}}_{\triangle}(16, l, ecf)$ (Fig. 6) where $l = 0$ or 1, and $ecf = ONE$ or QS or $QSPO$. The NPT graphs are calculated from simulation runs up to $T = 6400$ updates. We observe that graphs of NPT of PSN model set-ups $\mathcal{L}^{\mathrm{p}}_{\Box}(16, 0, ecf)$ with $ecf = ONE$, or QS, or $QSPO$ are almost identical, see (a) in Fig. 5. The same holds true for PSN model set-ups $\mathcal{L}^{\mathrm{p}}_{\triangle}(16, 0, ecf)$ with $ecf = ONE$, or QS, or $QSPO$, see (a) in Fig. 6. For each type of network connection topology the NPT graphs are constant for source loads λ smaller than the corresponding critical source loads λ_{c}. For source loads bigger than the corresponding critical source loads λ_{c} the graphs of NPT monotonically increase with the increase of source load values.

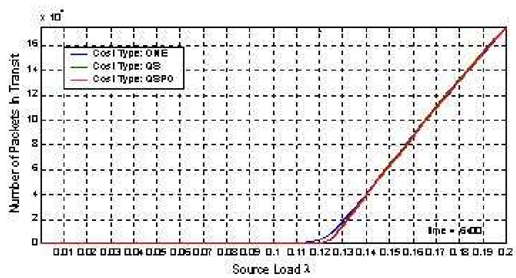

(a)

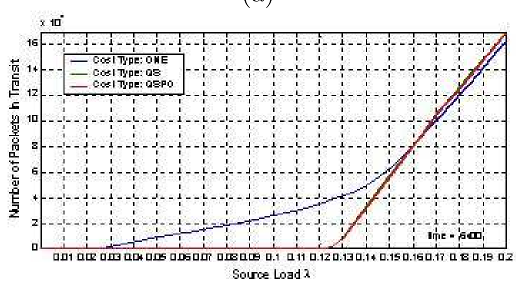

(b)

Fig. 5. Plots of *number of packets in transit (NPT)* of PSN model set-up with network connection topology $\mathcal{L}^{\mathrm{p}}_{\Box}(16, 0)$ in (a) and $\mathcal{L}^{\mathrm{p}}_{\Box}(16, 1)$ in (b) and edge cost function ONE blue graphs, QS green graphs and $QSPO$ red graphs, at simulation time $T = 6400$.

This qualitative behavior of the NPT graphs holds also true for the PSN model set-ups with network connection topologies $\mathcal{L}^{\mathrm{p}}_{\Box}(16, 1)$ and $\mathcal{L}^{\mathrm{p}}_{\triangle}(16, 1)$. By comparing the graphs of NPT of figure (a) with those of figure (b) in Fig. 5 and, respectively, in Fig. 6, we also notice that an addition of an extra link to the network connection topology $\mathcal{L}^{\mathrm{p}}_{\Box}(16, 0)$ and $\mathcal{L}^{\mathrm{p}}_{\triangle}(16, 0)$ has no effect on the graphs of NPT of PSN model set-ups using edge cost function

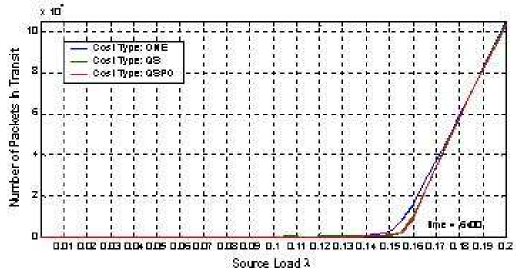

(a)

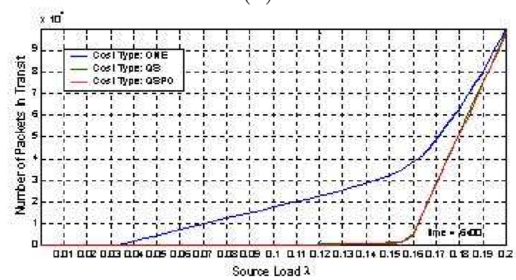

(b)

Fig. 6. Plots of *number of packets in transit (NPT)* of PSN model set-up with network connection topology $\mathcal{L}^{\mathrm{p}}_{\triangle}(16, 0)$ in (a) and $\mathcal{L}^{\mathrm{p}}_{\triangle}(16, 1)$ in (b) and edge cost function ONE blue graphs, QS green graphs and $QSPO$ red graphs, at simulation time $T = 6400$.

QS or *QSPO*. However, it has a significant effect on the *NPT* graphs in the case of PSN model set-ups using the edge cost function *ONE*. This is because the critical source loads λ_{c} of PSN model set-ups $\mathcal{L}^{\mathrm{p}}_{\square}(16, 1, ONE)$ and $\mathcal{L}^{\mathrm{p}}_{\triangle}(16, 1, ONE)$ are significantly smaller than those of PSN model set-ups $\mathcal{L}^{\mathrm{p}}_{\square}(16, 0, ONE)$ and $\mathcal{L}^{\mathrm{p}}_{\triangle}(16, 0, ONE)$. Furthermore, the NPT graphs of the PSN model set-ups $\mathcal{L}^{\mathrm{p}}_{\square}(16, 1, ONE)$ and $\mathcal{L}^{\mathrm{p}}_{\triangle}(16, 1, ONE)$ change their rate of increase twice. The first change of rate of increase (form zero to non-zero) corresponds to the transition from free-flowing state to the locally congested state of each instance of the PSN model set-up. The second change of rate of increase in the NPT graphs corresponds to the transition from the locally congested state to the globally congested state of each instance of the PSN model set-up. This can also be confirmed by seeing Fig. 2 in the case of the PSN model set-up $\mathcal{L}^{\mathrm{p}}_{\square}(16, 1, ONE)$.

The graphs of the network performance indicator *average delay time of all packets delivered* ($ADTPD$) as a function of source load λ of the PSN model set-ups $\mathcal{L}^{\mathrm{p}}_{\square}(16, l, ecf)$ and $\mathcal{L}^{\mathrm{p}}_{\triangle}(16, l, ecf)$, where $l = 0$ or 1, and $ecf = ONE$, or QS, or $QSPO$, are displayed, respectively, in Fig. 7 and

Fig. 8. By looking at the graphs in figures (a) of Fig. 7 and Fig. 8 we notice that for PSN model set-ups with undecorated network connection topologies, *i.e.* $\mathcal{L}^{\mathrm{p}}_{\Box}(16,0)$ and $\mathcal{L}^{\mathrm{p}}_{\triangle}(16,0)$, the graphs of $ADTPD$ behave qualitatively very similarly.

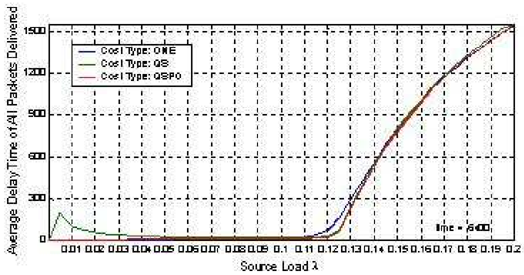

(a)

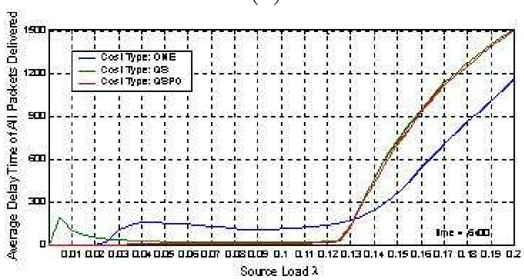

(b)

Fig. 7. Plots of *average delay time of all packets delivered (ADTPD)* of PSN model set-up with network connection topology $\mathcal{L}^{\mathrm{p}}_{\Box}(16,0)$ in (a) and $\mathcal{L}^{\mathrm{p}}_{\Box}(16,1)$ in (b) and edge cost function ONE blue graphs, QS green graphs and $QSPO$ red graphs, at simulation time $T = 6400$.

The same holds true for the PSN model set-ups with decorated network connection topologies, *i.e.* $\mathcal{L}^{\mathrm{p}}_{\Box}(16,1)$ and $\mathcal{L}^{\mathrm{p}}_{\triangle}(16,1)$. For the PSN model set-ups $\mathcal{L}^{\mathrm{p}}_{\Box}(16,0,ecf)$ and $\mathcal{L}^{\mathrm{p}}_{\triangle}(16,0,ecf)$, where $ecf = ONE$ or $QSPO$, the graphs of $ADTPD$ are constant for source loads λ smaller than the corresponding critical source loads λ_{c} and they increase monotonically with the increase of source load values for source loads λ larger than the corresponding critical source loads λ_{c}. For the PSN model set-ups $\mathcal{L}^{\mathrm{p}}_{\Box}(16,0,QS)$ and $\mathcal{L}^{\mathrm{p}}_{\triangle}(16,0,QS)$ the behavior of $ADTPD$ graphs is similar except for very small source load values. For these source load values each of the graphs of $ADTPD$ attains first its local maximum. This happens because for the PSN model set-ups using the edge cost function QS there are only few queuing packets for very small source load values. Thus, the costs of all paths are very similar and packets perform almost random walks on their routes from their sources to their destinations. This results in higher values of $ADTPD$

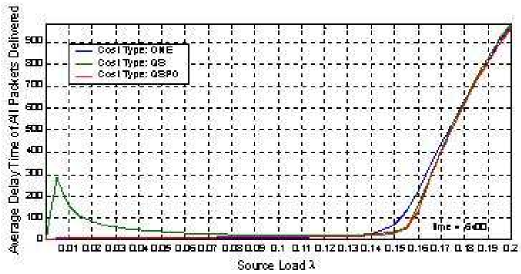

(a)

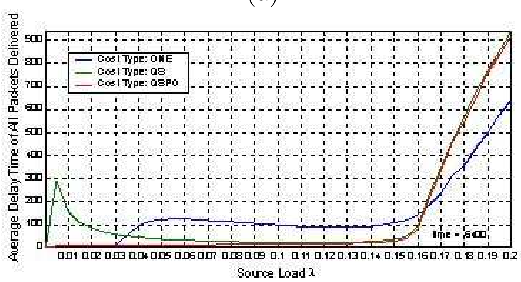

(b)

Fig. 8. Plots of *average delay time of all packets delivered (ADTPD)* of PSN model set-up with network connection topology $\mathcal{L}^{\mathrm{p}}_{\triangle}(16,0)$ in (a) and $\mathcal{L}^{\mathrm{p}}_{\triangle}(16,1)$ in (b) and edge cost function ONE blue graphs, QS green graphs and $QSPO$ red graphs, at simulation time $T = 6400$.

graphs for small source load values. With the increase of source load values there are more queuing packets in a network and the costs of the paths become more differentiated. Thus, packets are delivered more efficiently from their sources to their destinations and the values of $ADTPD$ graphs drop and stay almost constant for source loads λ smaller than λ_c.

By looking at the $ADTPD$ graphs in Fig. 7 and Fig. 8 we observe that an addition of an extra link has very little effect on $ADTPD$ graphs in the case of PSN model set-ups with edge cost function QS and $QSPO$ but it has significant effect in the case of PSN model set-ups with edge cost function ONE. In each of the $ADTPD$ graphs corresponding to either one of the PSN model set-ups with edge cost function ONE and network connection topology $\mathcal{L}^{\mathrm{p}}_{\square}(16,1)$ or $\mathcal{L}^{\mathrm{p}}_{\triangle}(16,1)$ the first increase happens for the source loads for which the local congestion at the end nodes of an extra link starts to build up. This can be seen also from the figures in Fig. 2 for PSN model set-up $\mathcal{L}^{\mathrm{p}}_{\square}(16,1,ONE)$. This increase is followed by the plateaus in $ADTPD$ graphs that correspond to the source loads at which the PSN model set-ups are only locally congested at the end nodes of the extra link. The second increase in $ADTPD$ graphs happens for source loads for which the PSN model set-ups become globally congested. The values of the source loads corresponding to the right hand side ends of the plateaus of $ADTPD$ graphs are closed to the ones at which *throughputs* attain their maximum and NPT graphs change their rates of increase for the second time.

In conclusion the network performance indicators *throughput*, *number of packets in transit* (NPT), and *average delay time of all packets delivered* ($ADTPD$) for the considered PSN model set-ups change significantly their qualitative and quantitative behaviors for source loads near the corresponding critical source loads λ_c. We observe that an addition of an extra link to the network connection topologies $\mathcal{L}^{\mathrm{p}}_{\square}(16,0)$ and $\mathcal{L}^{\mathrm{p}}_{\triangle}(16,0)$ has very little impact on the discussed aggregate measures of network performance in the case of PSN model set-ups using the edge cost function QS or $QSPO$, that is in the case of dynamic (adaptive) routing. However, such addition has a significant impact in the case of PSN model set-ups using the edge cost function ONE that is, in the case of static routing. For the analysis of the behaviors of other network performance indicators of aggregate type and how the addition of a larger number of extra links affects the performance of various PSN model set-ups , see [15,20,29–34] for the PSN model under consideration and for slightly different model see [9, 12, 28].

3.2. Spatio-temporal packet traffic dynamics near onset of congestion

By looking at the graphs of the network performance indicators discussed in the previous section one may be tempted to conclude that for PSN models set-ups with undecorated network connection topologies (*i.e.*, $\mathcal{L}^{\mathrm{p}}_{\square}(16,0)$ and $\mathcal{L}^{\mathrm{p}}_{\triangle}(16,0)$ packet traffic dynamics does not depend significantly on the edge cost function type. Also, one may think that the connectivity of the network connection topology (*i.e.*, network connection topology isomorphic to a square lattice vs. the one isomorphic to a triangular lattice) does not have a strong effect on packet traffic dynamics. Furthermore, by looking at the graphs of the discussed network performance indicators one may also be tempted to conclude that addition of an extra link to the network connection topologies $\mathcal{L}^{\mathrm{p}}_{\square}(16,0)$ and $\mathcal{L}^{\mathrm{p}}_{\triangle}(16,0)$ has no effect on packet traffic dynamics in PSN model set-ups using the edge cost function QS or $QSPO$ and it has only an effect when the edge cost function ONE is used instead. To verify all these hypotheses we examine spatio-temporal packet traffic dynamics for the discussed PSN model set-ups for source loads close to their respective critical source loads λ_c, that is near the phase transition points from congestion free states (free flowing network states) to the congested states of the networks.

Plots in Figs. 9, 10, 11, and 12 display spatial distribution of the outgoing queue sizes at nodes for various PSN model set-ups. The x- and y- axis coordinates of each plot denote the positions of switching nodes and z-axis denotes the number of packets in the outgoing queue of the node located at that (x, y) position. The header of each column of the table in each of the Figs. 9 to 12 and the parameters shown under each plot uniquely define the PSN model set-up, the simulation time, the values of critical source load λ_{c} and super-critical source load $\lambda_{\mathrm{sup-c}}$.

Looking at the plots in Fig. 9 and Fig. 10 we observe that the qualitative behavior of spatial distribution of outgoing queue sizes is very similar for PSN model set-up $\mathcal{L}^{\mathrm{p}}_{\Box}(16, l, ONE)$ and $\mathcal{L}^{\mathrm{p}}_{\triangle}(16, l, ONE)$ when, respectively, $l = 0$ or 1, and in each case the source load is λ_{c} or $\lambda_{\mathrm{sup-c}}$. When $l = 0$, in each instance of PSN model set-up the queue sizes are randomly distributed with large fluctuations. Increase in source load results in substantial increase of queue sizes and fluctuations among them (notice, the plots use different scales on z-axis). When $l = 1$, in each case of the PSN model set-up with edge cost function ONE, that is for $\mathcal{L}^{\mathrm{p}}_{\Box}(16, 1, ONE)$ and $\mathcal{L}^{\mathrm{p}}_{\triangle}(16, 1, ONE)$, the end nodes of an extra link become very quickly locally congested (see also plots in Fig. 11). The extra link provides a "short-cut" in packets traffic and many packets are being sent via routes passing through this link, regardless how big the outgoing queues are at the nodes to which this extra link attaches. When the edge cost function ONE is used the routing is static, hence, it does not have build in mechanism to avoid congested nodes of the network. Thus, this leads to the build up of local congestion for broad range of source load values (see plots in Fig. 11) on the time scale of our simulations before the networks become globally congested for higher source load values or longer time simulations. The build up of local congestion is responsible for changes in the graphs of network performance indicators discussed in the previous section. In particular, it is responsible for the plateaus observed in the graphs of *average delay time of all packets delivered* in Figs. 7 and 8. The discussed characteristics of the outgoing queue size distributions observed for λ_{c} and $\lambda_{\mathrm{sup-c}}$ are also observed in this type of distributions, respectively, for other sub-critical source load values and super-critical ones in PSN model set-ups $\mathcal{L}^{\mathrm{p}}_{\Box}(16, l, ONE)$ and $\mathcal{L}^{\mathrm{p}}_{\triangle}(16, l, ONE)$ when, respectively, $l = 0$ or 1 and L is different than 16.

From the plots in Fig. 9 and Fig. 10, as in the case of the discussed above PSN model set-ups using edge cost function ONE, we observe a random distribution of outgoing queue sizes in each PSN model set-up $\mathcal{L}^{\mathrm{p}}_{\Box}(16, 0, ecf)$ and $\mathcal{L}^{\mathrm{p}}_{\triangle}(16, 0, ecf)$, where $ecf = QS$, $QSPO$, and the source loads are λ_{c}. However, the differences in the magnitudes of the fluctuations of these queue sizes are smaller than those in the case of PSN model set-ups using the edge cost function ONE. This is because in the PSN model set-ups using dy-

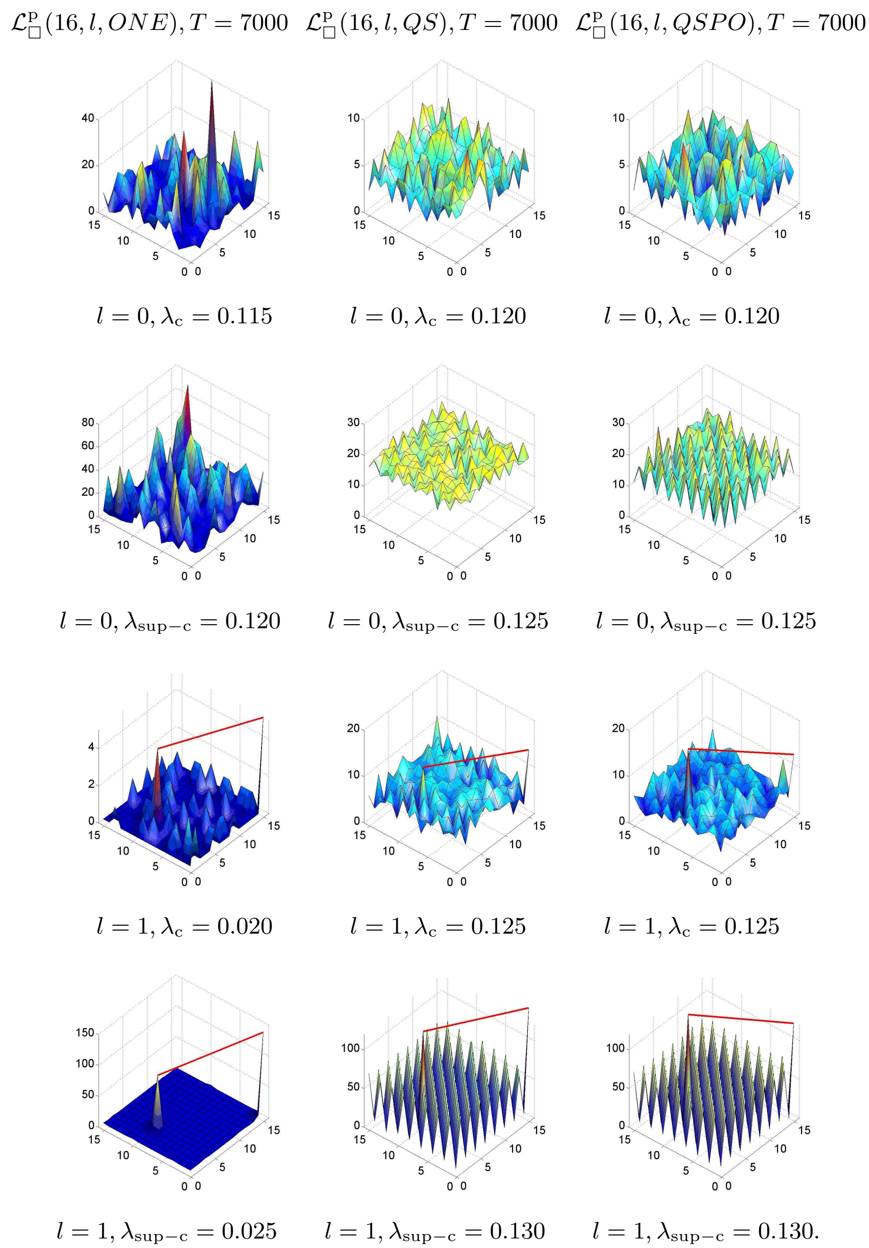

Fig. 9. Spatial distribution of outgoing queue sizes in PSN model set-ups $\mathcal{L}^{\mathrm{p}}_{\square}(16, l, ecf)$, with $l = 0$ or 1 and $ecf = ONE$, QS, $QSPO$, for critical source loads λ_{c} and super-critical source loads $\lambda_{\mathrm{sup-c}}$.

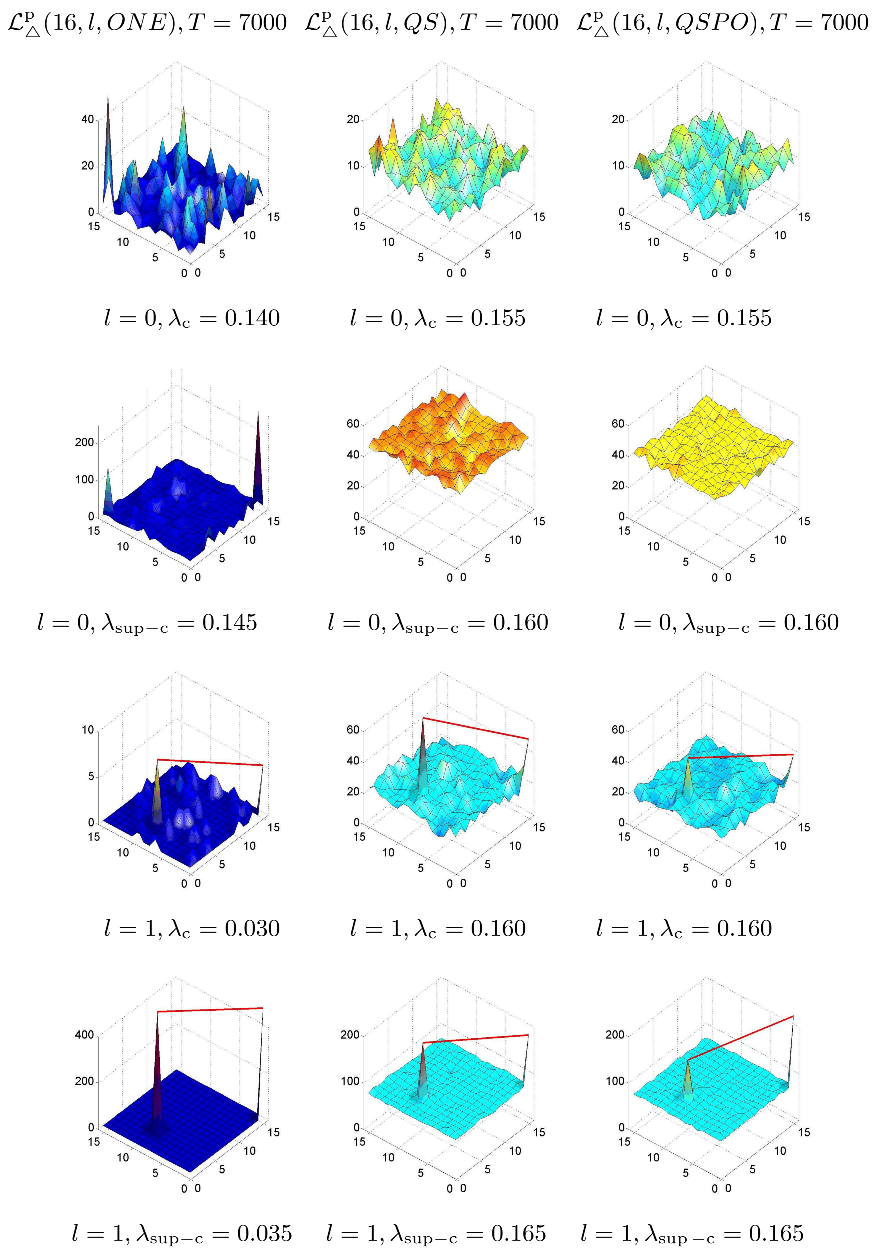

Fig. 10. Spatial distribution of outgoing queue sizes in PSN model set-ups $\mathcal{L}^{\mathrm{p}}_{\triangle}(16, l, ecf)$, with $l = 0$ or 1 and $ecf = ONE$, QS, $QSPO$, for critical source loads λ_{c} and super-critical source loads $\lambda_{\mathrm{sup-c}}$.

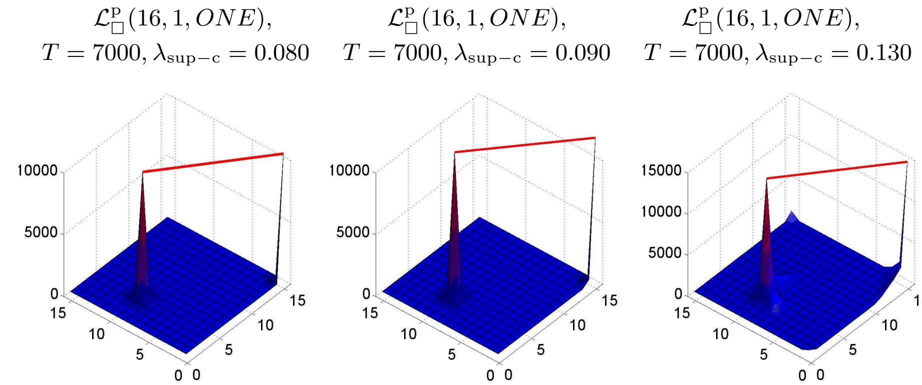

Fig. 11. Spatial distribution of outgoing queue sizes in PSN model set-up $\mathcal{L}^{\mathrm{p}}_{\Box}(16,1,ONE)$ for three different super-critical source loads $\lambda_{\mathrm{sup-c}}$.

namic edge cost function QS or $QSPO$ the adaptive routing tries to avoid congested areas of the network when routing the packets. Thus, this results in a more even distribution of packets among the outgoing queues. For the other sub-critical source load values in the PSN model set-ups $\mathcal{L}^{\mathrm{p}}_{\Box}(16,0,ecf)$ and $\mathcal{L}^{\mathrm{p}}_{\triangle}(16,0,ecf)$, where $ecf = QS$, $QSPO$, respectively, queue size distributions and fluctuations are qualitatively similar. However, we observe a significant qualitative difference between the distribution of outgoing queue sizes of the PSN model set-up $\mathcal{L}^{\mathrm{p}}_{\Box}(16,0,QSPO)$ and those of the set-ups $\mathcal{L}^{\mathrm{p}}_{\Box}(16,0,QS)$ and $\mathcal{L}^{\mathrm{p}}_{\triangle}(16,0,QS)$) and $\mathcal{L}^{\mathrm{p}}_{\triangle}(16,0,QSPO)$, when their respective $\lambda_{\mathrm{sup-c}}$ source loads are used, see plots of Fig. 9 and Fig. 10. We observe in the PSN model set-up $\mathcal{L}^{\mathrm{p}}_{\Box}(16,0,QSPO)$ with $\lambda_{\mathrm{sup-c}}$ (*i.e.*, in the congested state of the network) emergence of spatio-temporal self-organization in the sizes of the outgoing queues and formation of a pattern of peaks and valleys. At time $T = 8000$ this pattern is well developed across the whole network, see [35].

The pattern of peaks and valleys in the sizes of the outgoing queues emerges also in the PSN model set-up $\mathcal{L}^{\mathrm{p}}_{\Box}(16,0,QS)$ with $\lambda_{\mathrm{sup-c}}$, that is in the congested state of the network. However, the time scale on which this pattern emerges is much longer than the time scale on which it emerges in the PSN model set-up $\mathcal{L}^{\mathrm{p}}_{\Box}(16,0,QSPO)$, see [35]. Also, we notice that the differences among sizes of the neighboring peaks and valleys increase much faster with time in the PSN model set-up $\mathcal{L}^{\mathrm{p}}_{\Box}(16,0,QSPO)$ than the one with $\mathcal{L}^{\mathrm{p}}_{\Box}(16,0,QS)$, see [35]. This could imply that, when the edge cost function $QSPO$ is used, the cost component ONE is responsible for the observed qualitative differences in the evolution of the spatio-temporal packet traffic dynamics between the PSN model set-up $\mathcal{L}^{\mathrm{p}}_{\Box}(16,0,QSPO)$

$\mathcal{L}^{\mathrm{p}}_{\square}(16, l, QSPO)$, $T = 1000$ $\mathcal{L}^{\mathrm{p}}_{\square}(16, l, QSPO), T = 3000$ $\mathcal{L}^{\mathrm{p}}_{\square}(16, l, QSPO), T = 5000$

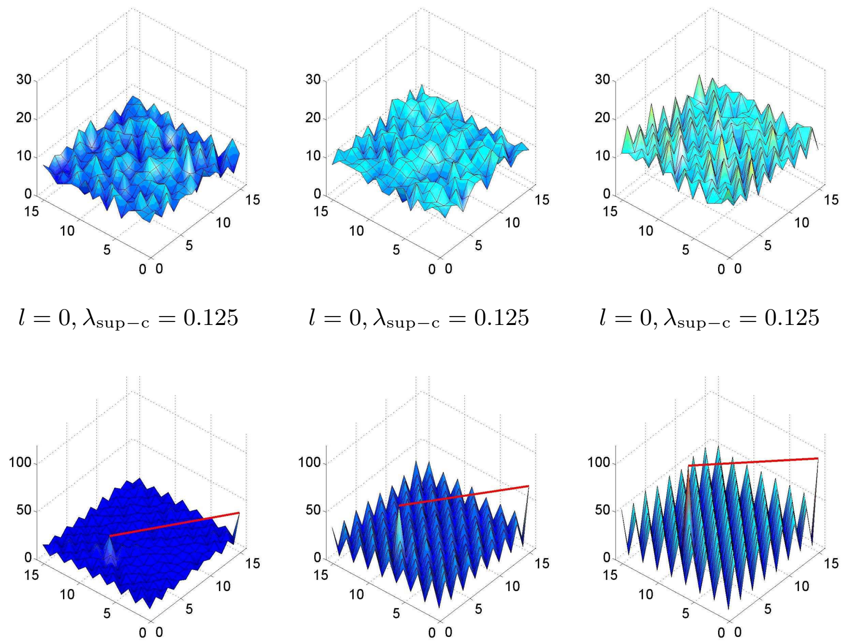

$l = 0, \lambda_{\mathrm{sup-c}} = 0.125$ $l = 0, \lambda_{\mathrm{sup-c}} = 0.125$ $l = 0, \lambda_{\mathrm{sup-c}} = 0.125$

$l = 1, \lambda_{\mathrm{sup-c}} = 0.130$ $l = 1, \lambda_{\mathrm{sup-c}} = 0.130$ $l = 1, \lambda_{\mathrm{sup-c}} = 0.130$

Fig. 12. Spatial distribution of outgoing queue sizes in PSN model set-up $\mathcal{L}^{\mathrm{p}}_{\square}(16, 0, QSPO)$ (first row) and in PSN model set-up $\mathcal{L}^{\mathrm{p}}_{\square}(16, 1, QSPO)$ (second row) for super-critical source loads $\lambda_{\mathrm{sup-c}}$ at various times.

and the one with $\mathcal{L}^{\mathrm{p}}_{\square}(16, 0, QS)$ in the congested state of each network. A similar behavior in these types of PSN model set-ups was observed for values of L other than 16 and other super-critical source load values. Thus, in the PSN model set-ups $\mathcal{L}^{\mathrm{p}}_{\square}(16, 0, QS)$ and $\mathcal{L}^{\mathrm{p}}_{\square}(16, 0, QSPO)$ in their congested states as the number of packets increases the pattern of peaks and valleys emerges in spite of the adaptive routing attempts to distribute the packets evenly among the outgoing queues. On the time scales of the performed simulations we have not observed the emergence of the pattern of peaks and valleys in the distributions of the outgoing queue sizes of the PSN model set-ups $\mathcal{L}^{\mathrm{p}}_{\triangle}(16, 0, QS)$ and $\mathcal{L}^{\mathrm{p}}_{\triangle}(16, 0, QSPO)$ in their congested states. In the case of these PSN model set-ups the queuing packets are distributed much more evenly (see plots in Fig. 10). Thus, the network connection topology connectivity in PSN models using adaptive routing plays an important role in the emergence of patterns in spatial distributions of packets among the queues.

Looking at the plots in Fig. 9 and Fig. 12 we see that adding an extra link to the network connection topology of each of the PSN model set-ups $\mathcal{L}^{\mathrm{p}}_{\square}(16,0,QS)$ and $\mathcal{L}^{\mathrm{p}}_{\square}(16,0,QSPO)$ speeds up a "peak-valley" pattern emergence in their congested states. This is also true for PSN model set-ups $\mathcal{L}^{\mathrm{p}}_{\square}(L,0,QS)$ and $\mathcal{L}^{\mathrm{p}}_{\square}(L,0,QSPO)$, $\mathcal{L}^{np}_{\square}(16,0,QS)$ and $\mathcal{L}^{np}_{\square}(16,0,QSPO)$ (where *np* in the superscript means non-periodic square lattice) when an extra link has other position and/or length and L is different from 16 (see [15, 33, 34] and [35]). Thus, in spite of the fact that the considered adaptive routings try to distribute packets evenly among the network nodes the influence of an extra link is stronger one by preventing this to happen and speeding up the "peak-valley" pattern formation. This is also true when instead of one extra link a relatively small number of extra links is added (see [15]). The speeding up of pattern formation happens because an extra link or small number of them provides a "short-cut in communication" among more distant nodes about the states of their outgoing queues that is about possible local congestions.

For PSN model set-ups with decorated (*i.e.*, with an extra link) periodic or non-periodic triangular network connection topologies and edge cost functions QS or $QSPO$ in the congested states of the networks we have not seen emergence of peak-valley patterns on the time scales of our simulations (see plots in Fig. 10). Recall that each periodic/non-periodic triangular lattice can be obtained from periodic/non-periodic square lattice by adding in a proper way a sufficient number of extra links. Thus, addition of many extra links to the network connection topologies $\mathcal{L}^{\mathrm{p}}_{\square}(L,0)$ and $\mathcal{L}^{np}_{\square}(L,0)$ prevents emergence of the peak-valley patterns in PSN model set-ups with dynamic edge cost functions QS or $QSPO$ in their congested states (see plots in Figs. 10 and [33]). Looking at the plots in Fig. 10 we observe rather small differences among the outgoing queue sizes in the congested states of the PSN model set-ups $\mathcal{L}^{\mathrm{p}}_{\triangle}(16,0,QS)$ and $\mathcal{L}^{\mathrm{p}}_{\triangle}(16,0,QSPO)$. These differences seem to be even smaller, when an extra link is added to the periodic triangular network connection topology, except of the two nodes to which the extra link is attached. These nodes attract much larger numbers of packets than other nodes. This results in the build up of local congestion at these nodes. In conclusion, the connectivity of network connection topology in the PSN model set-ups with dynamic edge cost QS or QSPO is responsible for the emergence or not of the peak-valley pattern in congested states of these networks.

4. Conclusions

We briefly described the PSN model of the OSI Network Layer (see for details [15, 20], and [21]) used in our study. We introduced definitions of the following aggregate measures of network performance *critical* *source load*, *throughput*, *number of packets in transit*, *average delay time of all packets delivered* [1–6,15]. We studied how these network performance indicators are affected by network connection topology type and static and adaptive routing algorithms. We observed that for all three PSN model set-ups $\mathcal{L}^{\mathrm{p}}_{\Box}(16, 0, ecf)$, where $ecf = ONE$ or QS or $QSPO$, the graphs of *throughput*, *number of packets in transit*, *average delay time of all packets delivered* are almost identical. However, there are significant differences in the spatial distributions of the outgoing queue sizes between the PSN model set-up $\mathcal{L}^{\mathrm{p}}_{\Box}(16, 0, ONE)$ and those with $\mathcal{L}^{\mathrm{p}}_{\Box}(16, 0, ecf)$, where $ecf = QS$, or $QSPO$, particularly, in the network congested states. These differences became even more significant when an extra link is added to the network connection topology $\mathcal{L}^{\mathrm{p}}_{\Box}(16, 0)$.

Our simulations showed that even small changes in network connection topology may significantly affect spatio-temporal packet traffic dynamics and that the changes in these dynamics may not be detected by various network performance indicators. For example, we noticed that addition of an extra link to a network connection topology isomorphic to a periodic square lattice or a periodic triangular lattice has no effect on the studied aggregate measures of performance of PSN model set-ups with adaptive routing algorithms (*i.e.*, using the dynamic edge cost function QS or $QSPO$). However, in the case of PSN model set-ups with network connection topology isomorphic to a periodic square lattice and edge cost function QS or $QSPO$ (adaptive routings) addition of an extra link speeds up significantly emergence of a peak-valley pattern among outgoing queue sizes in the networks congested states. On the time scale of our simulations, emergence of such patterns was not observed in congested states of PSN model set-ups with adaptive routings and decorated network connection topologies isomorphic to decorated periodic triangular lattices. In the case of PSN model set-ups with static edge cost function ONE (*i.e.*, in the case of static routing) the aggregate measures of network performance detected the changes in spatio-temporal packet traffic dynamics caused by addition of an extra link. Namely, they detected the rapid build up of local congestion at the nodes to which this extra link was attached.

In conclusion, our study shows that even small change in a network connection topology (addition of an extra link) may significantly affect spatio-temporal packet traffic dynamics regardless if the routing is static or dynamic. However, the nature of how it effects these dynamics depends on the connectivity of network connection topology coupled with edge cost function type (or routing algorithm type, static *vs.* adaptive). We observed that changes in these dynamics may or may not be detected by the considered network performance indicators of the aggregate type.

The presented investigation contributes to the growing research on complex dynamics of data communication networks [8–47] and dynamics of other complex networks [51–56]. Better understanding of these dynamics can result in improvements in design and operation of data communication networks.

A.T. L. acknowledges partial financial support from SHARCNET and NSERC of Canada. X.T. acknowledges partial financial support from Sharcnet and the University of Guelph. The authors thank B. Di Stefano, A. Gerisch and K. Maxie for helpful discussions. All simulations were run on SHARCNET (Shared Hierarchical Academic Research Computing Network) at the University of Guelph site.

REFERENCES

[1] W. Stallings, *High-Speed Networks: TCP/IP and ATM Design Principles,* Prentice Hall, Upper Saddle River, New Jersey 1998.

[2] T. Sheldon, *Encyclopedia of Networking & Telecommunications*, Osborne/McGrawHill, Berkeley, California 2001.

[3] A. Leon-Garcia, I. Widjaja, *Communication Networks*, McGraw-Hill, Boston 2000.

[4] J. Walrand, P. Varaiya, *High-Performance Communication Networks*, Academic Press, San Diego 2000.

[5] Y. Zheng, S. Akhtar, *Networks for Computer Scientists and Engineering*, Oxford University Press, New York 2002.

[6] P.D. Bertsekas, R.G. Gallager, *Data Network*s, Prentice Hall, Upper Saddle River, New Jersy 1992.

[7] Information Technology-Open System Interconnection-Basic Reference Model: The basic model, Recommendation X.200 of the ITU-TS, 1994. URL `http://www.itu.int/`

[8] T. Ohira, R. Sawatari, *Phys. Rev.* **E58**, 193 (1998).

[9] H. Fukś, A.T. Lawniczak, *Mathematics and Computers in Simulations*, **51**, 101 (1999).

[10] H. Fukś, A.T. Lawniczak, S. Volkov, *ACM Transactions on Modeling and Computer Simulation* **11**, 233 (2001).

[11] Z. Ren, Z. Deng, Z. Sun, D. Shuai, *Comput. Phys. Commun.* **141**, 247 (2001).

[12] A.T. Lawniczak, P. Zhao, A. Gerisch, B. Di Stefano, *IEEE Canadian Review* **39**, 23, Winter (2002).

[13] J. Yuan, K. Mills, *Journal of Research of NIST*, **107**, 179 (2002).

[14] M. Woolf, D.K. Arrowsmith, R.J. Mondragon, J.M. Pitts, *Phys. Rev.* **E66**, 056106 (2002).

[15] A.T. Lawniczak, A. Gerisch, B. Di Stefano, in *Science of Complex Networks*; J.F.F. Mendes *et al.* Eds., *AIP Conference Proc.*, **776**, 166 (2005).

[16] L. Kocarev, G. Vattay, *Complex Dynamics in Communication Networks*, Springer-Verlag, Berlin Heidelberg 2005.

[17] R.V. Solé, S. Valverde, *Physica A* **289**, 595 (2001).

[18] A. Arenas, A. Diaz-Guilera, R. Guimera, *Phys. Rev. Lett.* **86**, 3196 (2001).

[19] S. Gábor, I. Csabai, *Physica A* **307**, 516 (2002).

[20] A.T. Lawniczak, A. Gerisch, B. Di Stefano, *Proceedings of IEEE CCECE 2003-CCGEI 2003*, Montreal, Quebec, Canada (May/mai 2003) 001-004.

[21] A. Gerisch, A.T. Lawniczak, B. Di Stefano, *Proceedings of IEEE CCECE 2003-CCGEI 2003*, Montreal, Quebec, Canada (May/mai 2003) 001-004.

[22] A.T. Lawniczak, P. Zhao, B. Di Stefano, *Proceedings of the Third International DCDIS Conference on "Engineering Applications and Computer Algorithms"*, Guelph, Ontario, Canada, May 15-18, 2003, p. 390, Watam Press, 2003.

[23] I. Glauche, W. Krause, R. Sollacher, M. Grainer, *Physica A* **325**, 577 (2003).

[24] W. Krause, I. Glauche, R. Sollacher, M. Grainer, *Physica A* **338**, 633 (2004).

[25] S. Valverde, R.V. Solé, *Eur. Phys. J.* **B38**, 245 (2004).

[26] A.T. Lawniczak, A. Gerisch, K.P. Maxie, B. Di Stefano, *IEEE Proc. of "HPCS 2005: The New HPC Culture The 19th International Symposium on High Performance Computing Systems and Applications"*, Guelph, May 15-18, 2005, pp. 9.

[27] N. Gupte, B.K. Singh, T.M. Janaki, *Physica A* **346**, 75 (2005).

[28] A.T. Lawniczak, A. Gerisch, P. Zhao, B. Di Stefano, *Proceedings of the Third International DCDIS Conference on "Engineering Applications and Computer Algorithms*", Guelph, Ontario, Canada, May 15-18, 2003, p. 378, Watam Press, 2003.

[29] A.T. Lawniczak, A. Gerisch, K. Maxie, *Proceedings of the Third International DCDIS Conference on "Engineering Applications and Computer Algorithms"*, Guelph, Onatrio, Canada, May 15-18, 2003, 384, Watam Press, 2003.

[30] A.T. Lawniczak, K.P. Maxie, A. Gerisch, *Proceedings of IEEE CCECE 2004-CCGEI 2004,* Niagara Falls, Ontario, Canada (May/mai 2004), 2429-2432, 2004.

[31] A.T. Lawniczak, K.P. Maxie, A. Gerisch, *Proceedings of IEEE CCECE 2004-CCGEI 2004*, Niagara Falls, Ontario, Canada (May/mai 2004), 2421-2424, 2004.

[32] K.P. Maxie, A.T. Lawniczak, A. Gerisch, *Proceedings of IEEE CCECE 2004-CCGEI 2004*, Niagara Falls, Ontario, Canada (May/mai 2004), 2433-2436, 2004.

[33] A.T. Lawniczak, K.P. Maxie, A. Gerisch, Springer-Verlag, *LNCS* **3305**, 325, 2004.

[34] K.P. Maxie, A.T. Lawniczak, A. Gerisch, *Proceedings of IEEE CCECE 2004-CCGEI 2004*, Niagara Falls, Ontario, Canada (May/mai 2004), 2425-2428, 2004.

[35] A.T. Lawniczak, X. Tang, *Eur. Phys. J.* **B50**, 231 (2006), `http://arxiv.org/abs/nlin.AO/0510070`

[36] A.T. Lawniczak, X. Tang, to appear in *International Journal of Unconventional Computing*, 2006.

[37] M. Takayasu, H. Takayasu, T. Sato, *Physica A*, **233**, 824 (1996).

[38] A.Y. Tretyakov, H. Takayasu, M. Takayasu, *Physica A*, **253**, 315 (1998).

[39] S. Valverde, R.V. Solé, *Physica A* **312**, 636 (2002).

[40] S. Maniccam, *Physica A* **321**, 653 (2003).

[41] S. Maniccam, *Physica A*, **331**, 669 (2004).

[42] D.K. Arrowsmith, R.J. Mondragon, M. Woolf, in *Complex Dynamics in Communication Networks*, Eds. L. Kocarev, G. Vattay, Springer-Verlag, Berlin Heidelberg, 2005, p.127.

[43] G. Mukherjee, S.S. Manna, *Physica A* **346**, 132 (2005).

[44] L. Zhao, Y-Ch. Lai, K. Park, N. Ye, *Phys. Rev.* **E71**, 026125 (2005).

[45] Z. Ren, Z. Deng, Z. Sun, *Comput. Phys. Commun.* **144**, 310 (2002).

[46] J. Yuan, K. Mills, in *Complex Dynamics in Communication Networks*, Eds. L. Kocarev, G. Vattay, Springer-Verlag, Berlin Heidelberg, p. 191, 2005.

[47] P. Echenique, J. Gómez-Gardeñes, Y. Moreno, *Europhys. Lett.* **71** (2), 325 (2005).

[48] `http://www.ist-intermon.org/index.html`

[49] `http://www.ist-intermon.org/overview/publications.html`

[50] S. Boccaletti, V. Latora, Y. Moreno, M. Chavez, D.-U. Hwang, *Phys. Rep.* **424**, 175 (2006).

[51] P. Baldi, P. Frasconi, P. Smyth, *Modeling the Internet and the Web, Probabilistic Methods and Algorithms*, John Wiley & Sons Ltd, West Sussex, England, 2003.

[52] S.N. Dorogovtsev, J.F.F. Mendes, *Evolution of Networks, From Biological Nets to the Internet and WWW*, Oxford University Press, Oxford, UK, 2003.

[53] R. Pastor-Satorras, A. Vespignani, *Evolution and Structure of the Internet, A Statistical Physics Approach*, Cambridge University Press, Cambridge, UK, 2004.

[54] R. Pastor-Satorras, M. Rubi, A. Diaz-Guilera, Eds., *Statistical Mechanics of Complex Networks*, *Lecture Notes in Physics*, Berlin-Heidelberg-New York 2003.

[55] E. Ben-Naim, H. Frauenfelder, Z. Toroczkai, Eds., *Complex Networks*, *Lecture Notes in Physics*, Berlin Heidelberg New York, 2004.

[56] J.F.F. Mendes, S.N. Dorogovtsev, A. Povolotsky, F.V. Abreu, J.G. Oliveira, Eds., *Science of Complex Networks*, *AIP Conference Proc.*, **776**, 2005.